

EUROPEAN ORGANIZATION FOR NUCLEAR RESEARCH
CERN - AB DEPARTMENT

AB-Note-2004-005 BT (Rev.2)

TS-Note-2004-001 DEC (Rev. 2)

SPS Extraction Kicker Magnet Cooling Design

M. Timmins, A. Bertarelli, J. Uythoven, E. Gaxiola

Abstract

The document describes the various steps taken in the design, tests and simulations of a new cooling system for the SPS extraction kicker magnets for points LSS4 and LSS6.

Geneva, Switzerland
January 2004

Table of Contents

1. INTRODUCTION.....	1
2. DESIGN	1
2.1 Original magnet concept.....	1
2.2 Conceptual cooling design.....	2
2.3 Material choice for the heat conductor	3
2.4 Heat conductor design:	3
3. THERMAL SIMULATIONS.....	4
3.1 Introduction	4
3.2 General modelling conditions and assumptions.....	4
3.3 Design Space® model, input power values and boundary conditions	4
3.3.1 Results.....	5
3.4 Conclusion of thermal calculations.....	6
3.5 Temperature diagnostic device and simulations	6
4. COOLING TEST BENCH.....	8
4.1 Introduction	8
4.2 Cooling test bench design	8
4.3 Design Space® simulations	8
4.3.1 Model, boundary conditions and power input values	8
4.3.2 Results.....	9
4.4 Comparison of simulations and measurements.....	9
4.5 Ansys® simulations.....	10
4.5.1 Model, boundary conditions and power input value	10
4.5.2 Results.....	10
4.5.3 Time constants	11
5. MACHINE MEASUREMENTS.....	12
6. CONCLUSIONS AND DISCUSSION.....	12
7. ACKNOWLEDGEMENT	13
APPENDIX A: ALUMINIUM NITRIDE CHARACTERISTICS	14
APPENDIX B: HEATING TIME CONSTANTS	15
Distribution list	16

List of figures

Figure 1 <i>MKE magnet cross section</i>	1
Figure 2 <i>MKE magnet front view</i>	2
Figure 3 <i>Heat dissipation within the ferrite</i>	2
Figure 4 <i>Heat absorber plates</i>	3
Figure 5 <i>Heat inducted area</i>	4
Figure 6: <i>Design Space® model with cooling system</i>	5
Figure 7 <i>Design space results with cooling system</i>	6
Figure 8 <i>PT100 probe installation</i>	6
Figure 9 <i>Design Space® model used for calculating the temperature interlock value</i>	7
Figure 10 <i>Design Space® results graph for interlock temperature value</i>	7
Figure 11 <i>Photos of the cooling test bench and the probes position</i>	8
Figure 12 <i>Cooling test bench simulation results for three power input values (1,2 and 3 corresponding to 0.2875, 0.6 and 0.85 kW/m). The frame structure was only removed for better visualisation of the results.</i>	9
Figure 13 <i>Comparison of simulations and measurements</i>	10
Figure 14 <i>Ansys® model</i>	10
Figure 15 <i>Ansys® results</i>	11
Figure 16 <i>Measured kicker field strength for the MKQH kicker magnet and the MKE kicker magnet as a function of the measured MKE temperature.</i>	12

List of tables

Table 1 <i>Material characteristics used in the Design Space® model</i>	4
Table 2 <i>Temperature comparison between Ansys® and Design Space® results</i>	11

1. INTRODUCTION

For the SPS extraction kicker magnet upgrade, the beam induced heating of the ferrites above the Curie temperature has to be avoided. A cooling system has been designed and incorporated into an existing extraction kicker magnet and will maintain the ferrites below its Curie temperature (125 °C) during nominal CNGS and LHC operation.

2. DESIGN

2.1 Original magnet concept

The existing MKE magnets are built with approximately 230 kg of ferrite core and approximately 70 kg of Aluminium (figure 1). The magnet is 1.7 m long and split into 7 cells (figure 2), each cell consists of 3 ferrites positioned to form a “C” shape. The original magnet was mostly cooled by radiation, as there is very little path for conduction through materials to the surrounding of the vacuum tank. This conduction aspect was improved to lower the ferrite temperature.

- 1 - Alignment device
- 2 - Frame structure
- 3 - Beam gap
- 4 - Vacuum tank
- 5 - “C” core

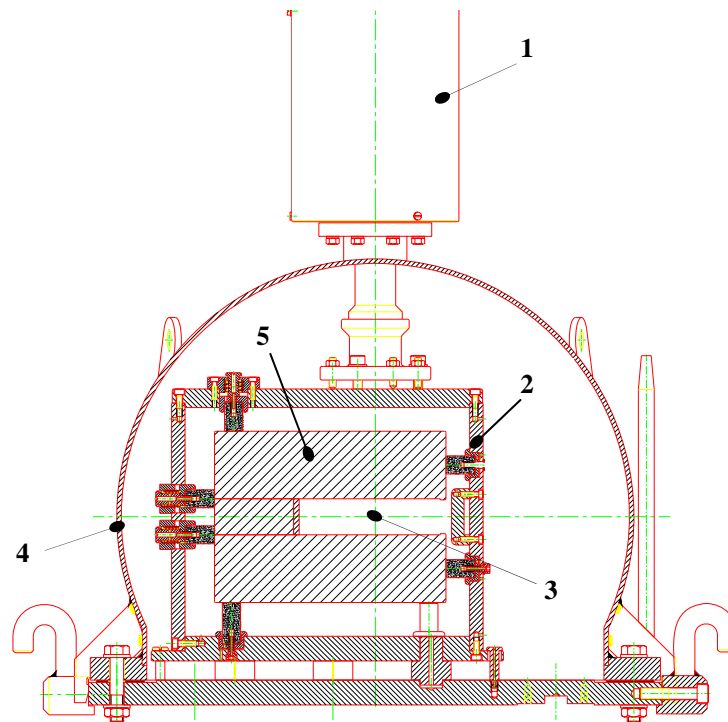


Figure 1 MKE magnet cross section

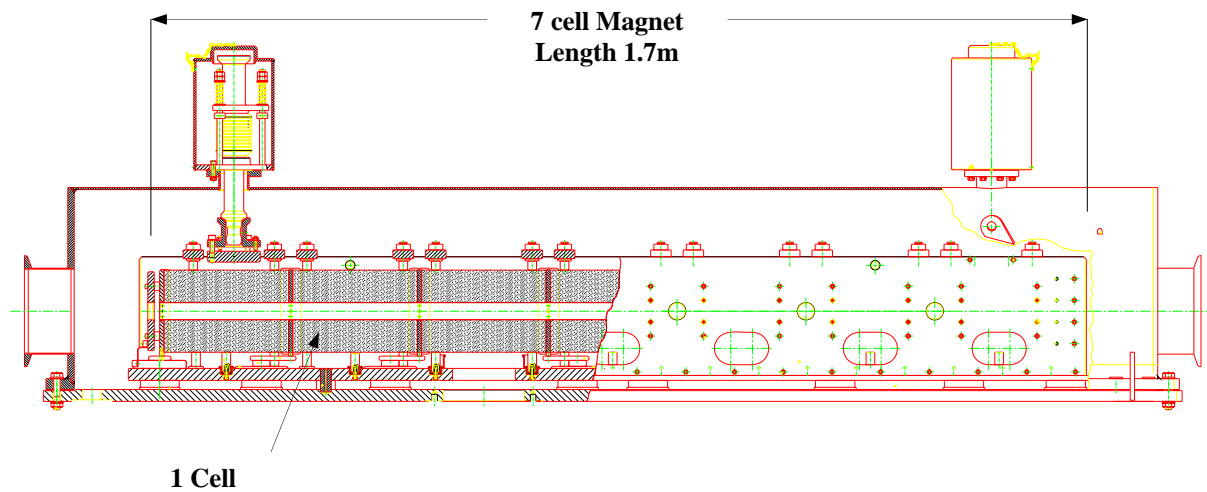


Figure 2 MKE magnet front view

2.2 Conceptual cooling design

To improve the heat evacuation from the ferrites it would have been ideal to insert a heat conductor inside the gap and capture the heat at the source before it spreads inside the ferrite. This would require an increase of the aperture size, which would reduce the kick strength of the magnet. Therefore, taking into account all the mechanical and electromagnetic field constraints the most appropriate place to insert a heat absorber is above the top ferrite and underneath the lower ferrite (*fig 3*).

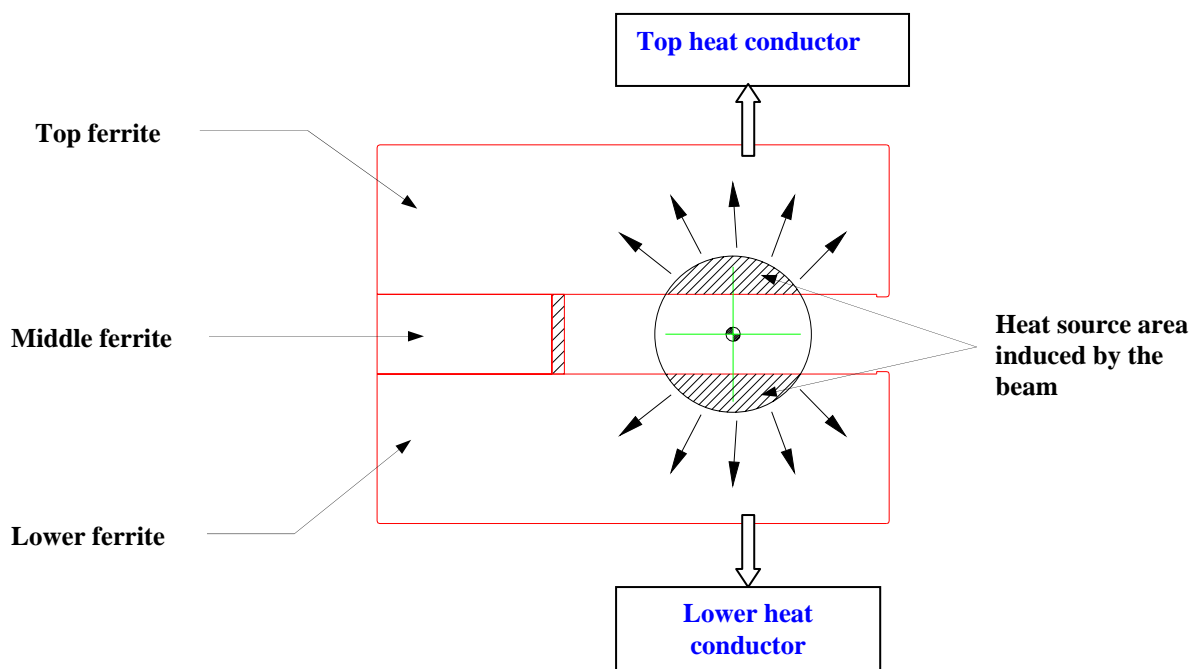


Figure 3 Heat dissipation within the ferrite

2.3 Material choice for the heat conductor

The heat conductor must be highly thermal conductive for evacuating the heat but also compatible with the HV (High Voltage) constraints given by the ferrites. Therefore electrically conductive materials are excluded. The material properties must be the following:

- Good electrical resistivity
- Good thermal conductivity
- Low degassing rate in ultra high vacuum
- Good mechanical strength

Two materials stood out when looking at these constraints:

- Aluminium nitride (AlN)
- Beryllium oxide (BeO)

As beryllium oxide is a highly toxic material, Aluminium Nitride was chosen for this application.

The material characteristics of Aluminium Nitride can be found in Appendix A.

2.4 Heat conductor design:

The basics of the conductor design consists of a series of two aluminium nitride plates per cell resting on top and underneath the ferrites, equipped with a water-cooling circuit as shown in figure 4. To guarantee a good mechanical contact and heat exchange between the ferrites and the plates, a spring-loaded pad applies a constant force of 200 N.

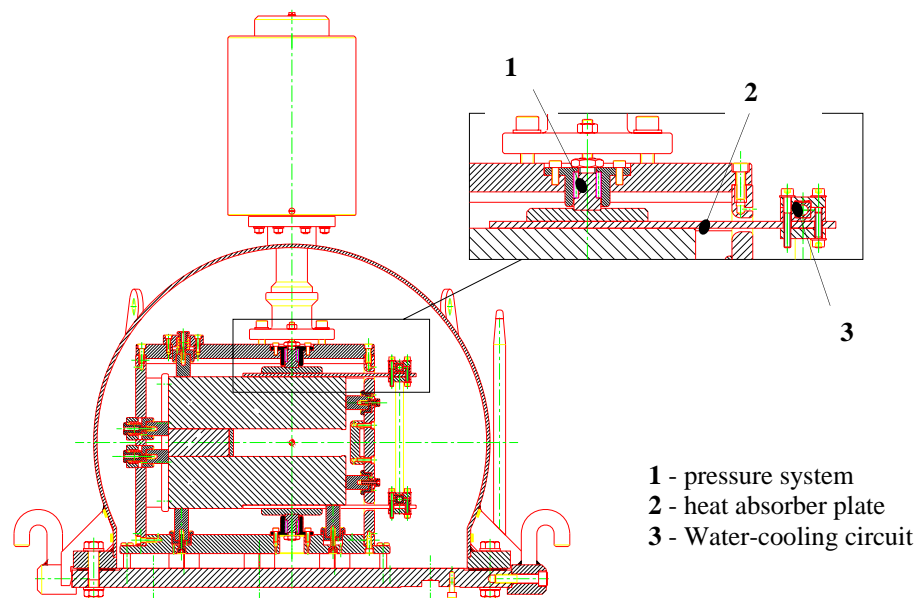


Figure 4 *Heat absorber plates*

3. THERMAL SIMULATIONS

3.1 Introduction

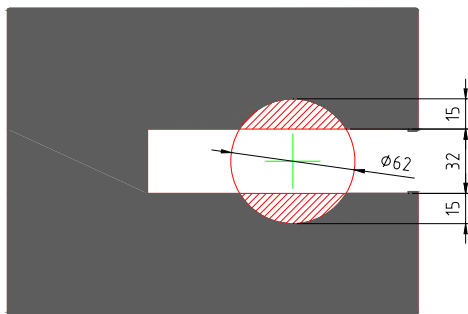
The design of the cooling system was made around the existing mechanical and electrical constraints. Adapting a simple cooling system to an existing structure had to be simulated to know if the resulting operational range of temperatures would be acceptable.

As the predominant means of cooling the magnet in our design is conduction, radiation is neglected in the calculations. (In paragraph 3.3.2 this is confirmed with a simple radiation power calculation). The programme Design Space[®] was used to carry out the calculations.

3.2 General modelling conditions and assumptions

The following model assumptions and conditions applied:

- 1 / 7th of the total magnet length, equivalent to 1 cell, was modelled (0.23m).
- Design Space[®] is limited to steady state calculations.
- Only thermal conduction is taken into account
- All undefined surfaces are considered as adiabatic.
- Surface contacts between parts are seen as perfect (100% contact).
- Power input: as shown in figure 5.
- Material characteristics: as shown in table 1.



CNGS beam intensity is given in kW/m
Design Space power values are given in W/m³

- CNGS beam power: **0.33 kW/m**
- Model length: **230 mm**
- Power in model: 330W x 0.23m = **76 W**
- Area submitted to this power in the model: **2.6.10⁵ mm³**
- Power in model: 76/2.6.10⁵ = **2.9.10⁻⁴ W/m³**

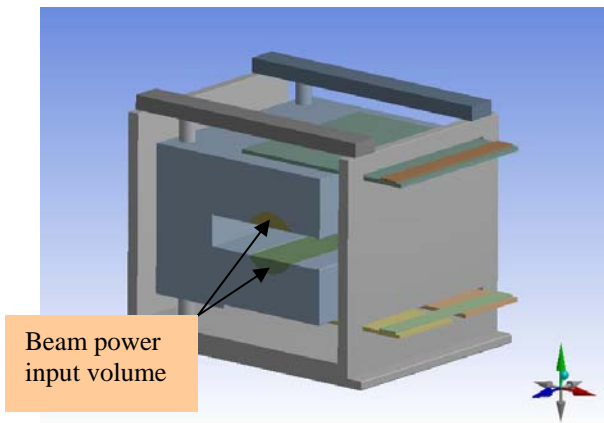
Figure 5 Heat induced area

Table 1 Material characteristics used in the Design Space[®] model.

	FUNCTION	THERM. CONDUCT. W/m.K	SPEC. HEAT J/Kg.K	DENSITY Kg/dm ³
FERRITE (Ferroxcube[®] 8C11)	MAGNET CORE	3.5	750	5
ALUMINIUM ALLOY (6082)	MAGNET FRAME	170	875	2.7
ALUMINIUM OXIDE (CERAMIC)	INSULATOR SPACERS	25	880	3.5
ALUMINIUM NITRIDE (AIN)	COOLING PLATES	180	738	3.3
COPPER ALLOY	WATER CIRCUIT	400	385	8.3

3.3 Design Space[®] model, input power values and boundary conditions

The geometry as shown in figure 6 was modelled with AutoCAD 3D tools and transferred as a “sat” file to Design Space[®]. The ferrite C core was modelled as one part instead of 3 parts. The two cooling plates are modelled with two stripes of copper on their extremities at constant temperature simulating the water circuit.



Input parameter:

- Beam power: $2.9 \cdot 10^{-4} \text{ W/m}^3$

Boundary condition:

- Temperature on the copper strips: 25°C

Figure 6: Design Space® model with cooling system.

3.3.1 Results

The results in figure 7 show that our maximum temperature in the model is 86°C . The average temperature on the outside of the frame is about 63°C .

The radiation between the frame and the vacuum tank can be estimated by using Boltzmann's formula:

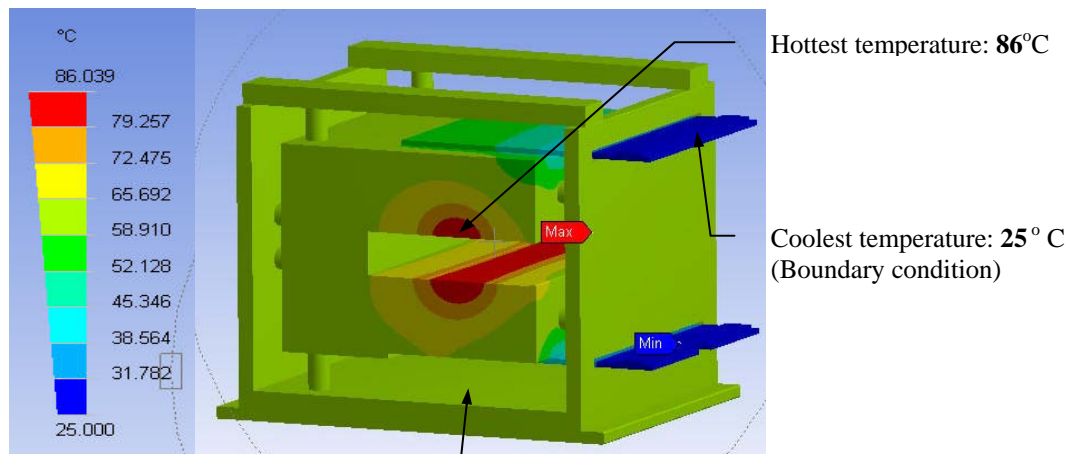
$$R(W) = S1 \times B \times (T1^4 - T2^4) \left/ \left[\frac{1}{E1} + \frac{(1 - E2) \times S1}{E2 \times S2} \right] \right.$$

$S1 = 1.2 \text{ m}^2$	$S2 = 2.7 \text{ m}^2$
$T1 = 333 \text{ K}$	$T2 = 25^\circ\text{C} = 298 \text{ K}$
$E1 = 0.05$	$E2 = 0.7$
$B = 5.67 \text{ E-8 Wm}^{-2}\text{K}^{-4}$	

With the frame at 63°C and the tank at 25°C the result is:

$$R(W) = 14.86 \text{ W / magnet or } 14.86 / 7 = 2.12 \text{ W /cell.}$$

This radiation power has to be compared to 76 W beam power initially injected into the model and represents 2% of the total power and can thus be neglected. The same rule applies to the radiated power from the ferrites to the frame where the temperature difference is even lower.



Average Temperature on the frame: $\sim 63^\circ\text{C}$

Figure 7 Design space results with cooling system

3.4 Conclusion of thermal calculations

Keeping in mind the various assumptions made in the model, the highest temperature (86°C) gives a good idea of how efficient the design could be. Taking into account the ferrites Curie temperature (125°C), the cooling was considered sufficient. Therefore the conceptual design was approved.

3.5 Temperature diagnostic device and simulations

For diagnostics and protection reasons a temperature probe (Pt100) is installed on the magnet. It is resting inside a ceramic insulator on the front part area of the ferrite as shown in figure 8. This probe is measuring a temperature lower than the highest temperature in the ferrite due to its position. The relation between these two temperatures can be calculated with Design Space® model as shown in figure 9.

- 1 - Pt100 probe
- 2 - Probed area
- 3 - Ceramic spacer
- 4 - Hottest area

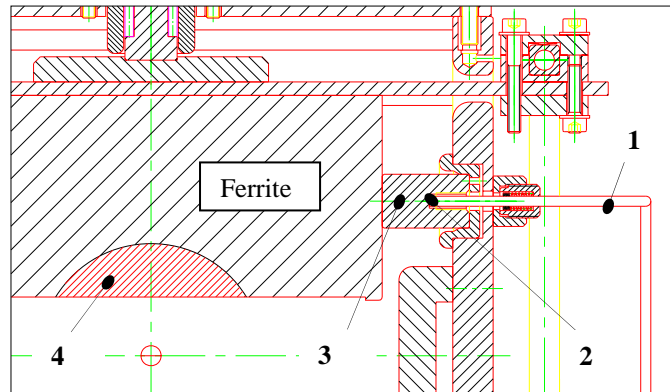
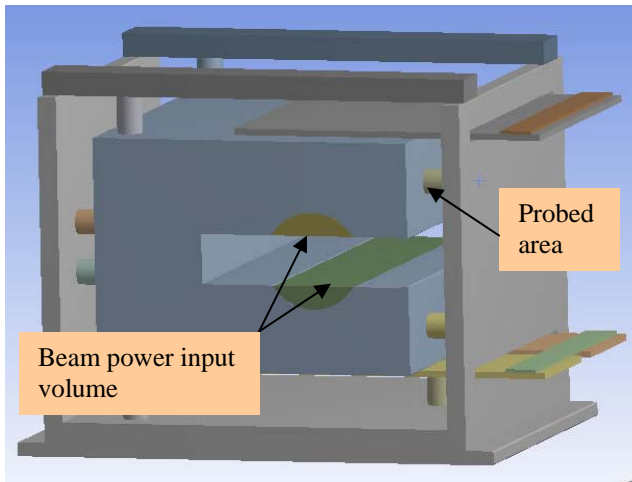


Figure 8 PT100 probe installation

The model was used for two different beam power input values (0.2 kW/m and 0.85 kW/m), as shown in figure 9. The resulting temperatures in relation to the power are shown in figure 10.



Input parameter:

- Beam power: $1.769 \cdot 10^{-4} \text{ W/m}^3$
- Beam power: $7.519 \cdot 10^{-4} \text{ W/m}^3$

Boundary condition:

- Temperature on the copper strips: 25°C

Figure 9 Design Space® model used for calculating the temperature interlock value

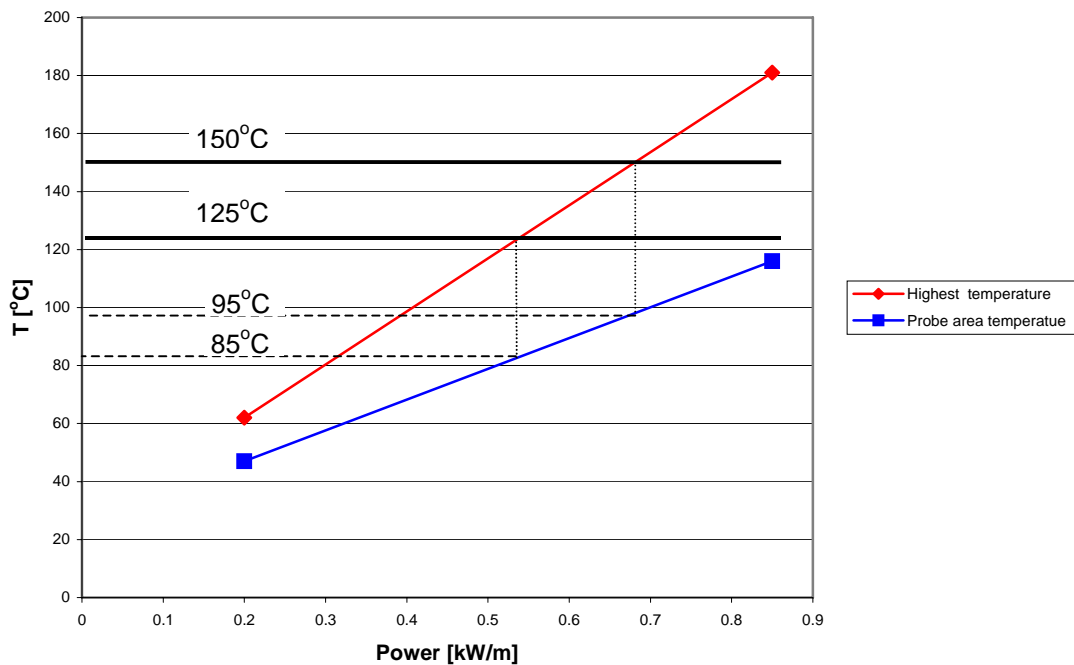


Figure 10 Design Space® results graph for attributing the interlock temperature value

The temperature at which the magnet will mechanically start to deteriorate is given by the maximum value at which the various materials can expand to, without generating high internal mechanical stress. Originally the MKE kicker magnets were designed to withstand 150°C , which corresponds to the bake out temperature to which they were submitted before installation. Therefore we decided to conserve this temperature as our ultimate limit. As shown on Figure 10, for a temperature of 150°C in the hottest spot of the model we have 95°C around the probed area. The interlock temperature for the ferrites Curie temperature is given for 125°C which corresponds to 85°C on the probe.

4. COOLING TEST BENCH

4.1 Introduction

The results of the thermal simulations established the main guidelines for the final design but before equipping the magnets with a cooling system it was preferable to confirm these promising results by building a test bench, reproducing a short version of the magnet, submitted to a heat source and cooled in the same way as the series magnets.

4.2 Cooling test bench design

The test bench is made of one complete magnet cell (1/7th of the total length) equipped with the cooling system as in the new magnet design and placed in a vacuum tank. Two titanium bars are placed inside the gap in contact with the top and lower ferrite and are ohmically heated by a current source outside of the vacuum tank. Four temperature probes are installed around the ferrite core for temperature measurements as shown in figure 11.

- Top probe (should be the coolest part of the ferrite)
- Front probe (equivalent area to the temperature diagnostic device in the magnet)
- Cooling plate probe (this probe is half way between the cooling circuit and the ferrite)
- Side probe (should be the hottest part of the ferrite as it is very close to the heating bars)

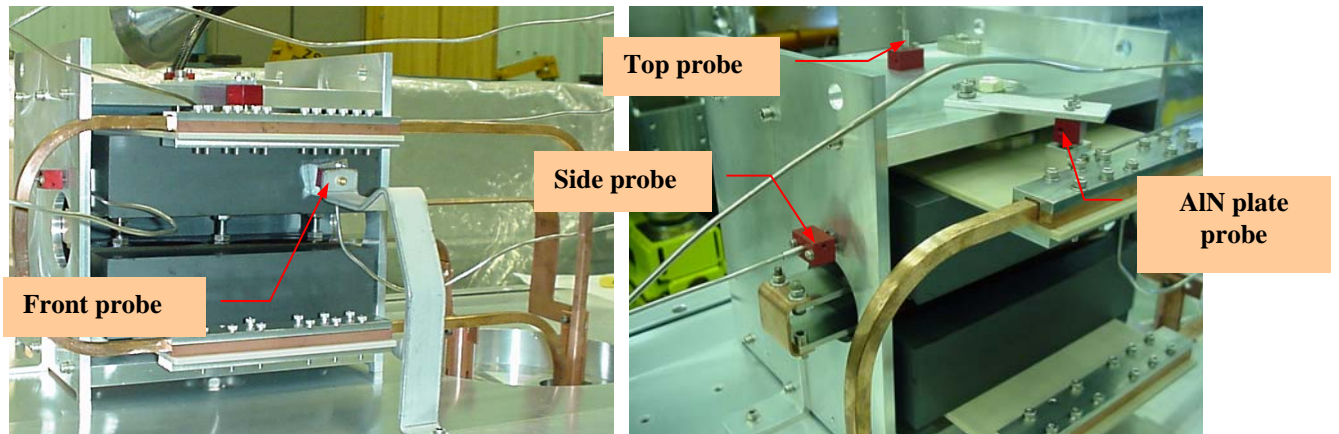


Figure 11 Photos of the cooling test bench and the probe's position

4.3 Design Space® simulations

To compare correctly the measured and the simulated data of the test bench model, a new Design Space® model, identical to the test bench construction was created and submitted to identical power values as in the test bench.

4.3.1 Model, boundary conditions and power input values

This new model corresponds to the aluminium box structure around the “C” shaped ferrites with two titanium bars positioned inside the gap acting as heating devices. (The aluminium

nitride plates remain identical to the previous model with the copper strips at a constant temperature of 25°C). Three areas will be probed on this model corresponding to the side, top and front probes positioned around the test bench.

4.3.2 Results

The Design Space® simulation results in figure 13 are given for three different power values. The highest temperature found in this model for 0.2875 kW/m is 79.5°C and by comparing this temperature with the 86°C found for 0.33 kW/m in the previous Design Space® model we notice how little difference there is due to the geometry changes: they are within 4% (taking into account the difference in powers).

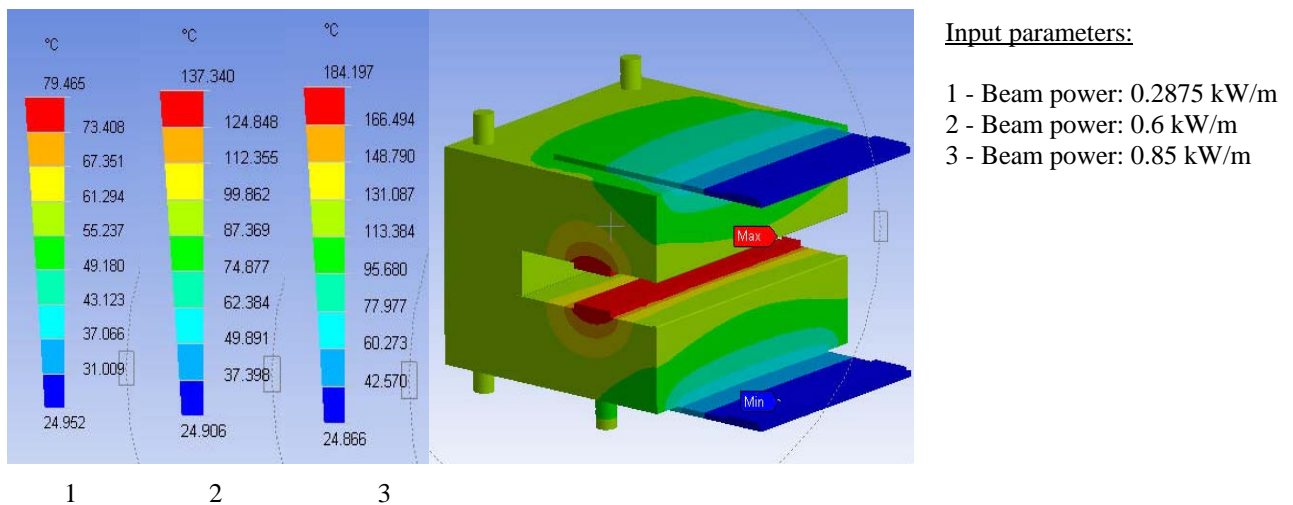


Figure 12 Cooling test bench simulation results for three power input values (1, 2 and 3 corresponding to 0.2875 , 0.6 and 0.85 kW/m). The frame structure was removed for better visualisation of the results only.

4.4 Comparison of simulations and measurements

In figure 14 the solid lines are the simulated temperatures and are compared to the dotted measured test bench temperatures. It shows a fairly good agreement between the two side probes: only a few degrees difference even at high powers. This is very promising as the side probe measures the temperature closest to the heat source

Nevertheless, the heat distribution within the rest of the ferrite seems to be much more optimistic in our calculations relative to the measured ones.

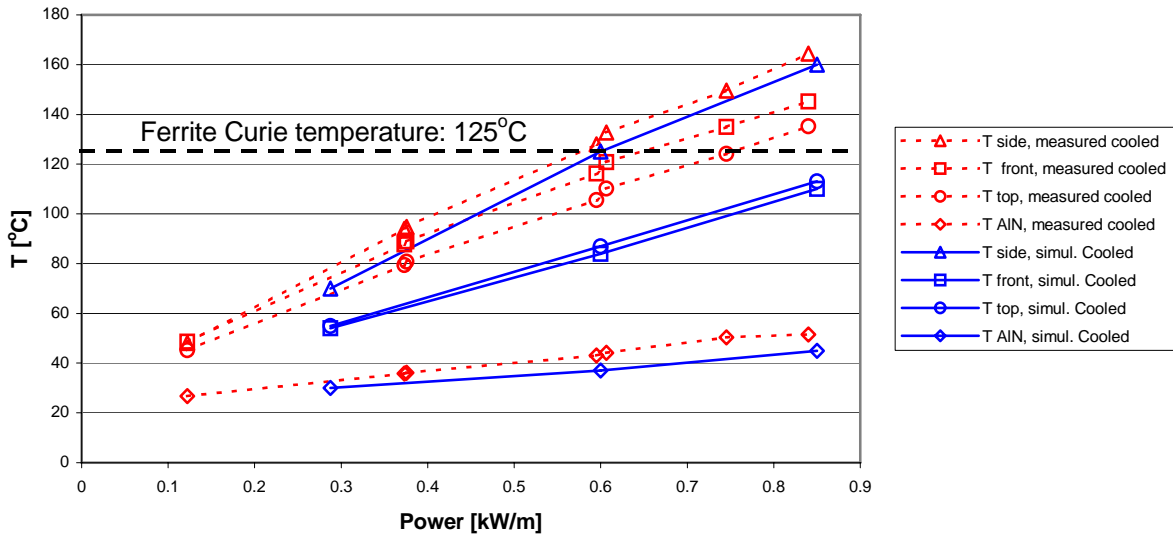


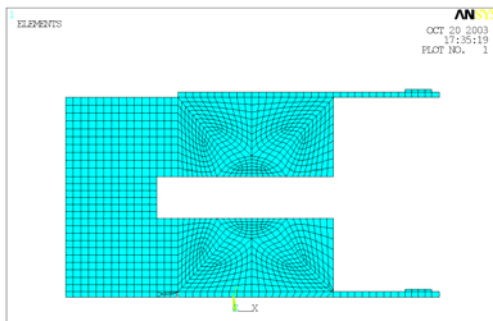
Figure 13 Comparison of simulations and measurements

4.5 Ansys® simulations

To verify that the disagreement mentioned above is not caused by finite element analysis problems, like non convergence or meshing defects, identical simulations were carried out with the programme Ansys®.

4.5.1 Model, boundary conditions and power input value

The model calculated with Ansys®, as shown in figure 14, corresponds to the calculation carried out with Design Space® as reported in paragraph 3.3.2 i.e. a 2D slice of the Design Space® model without the frame structure and the ceramic spacers. 2D modelling allows smaller meshing and calculations are faster. The material characteristics are identical to the previous model and the calculations were done in transient state to compare time constants with those measured with the test bench.



Transient calculation

Power input: **0.3 kW/m**

Boundary conditions: **25 °C** on the extremities of the Aluminium nitride plates

Figure 14 Ansys® model

4.5.2 Results

The two curves in figure 16 represent the relation between the hottest area and the diagnostic device area temperature, as done with the Design Space® results. The darker colored line

describes the hottest area and reaches an equilibrium temperature of $77\text{ }^{\circ}\text{C}$ and the other line describes the diagnostic device and reaches a temperature of $52\text{ }^{\circ}\text{C}$. The temperature rise in the two models differs by **10%**, which is acceptable.

Table 2 Temperature comparison between Ansys® and Design Space® results

	Power (kW/m)	Hottest spot temp. ($^{\circ}\text{C}$)	Device area temp. ($^{\circ}\text{C}$).
Ansys®	0.3	77	52
Design Space®	0.3	80	55

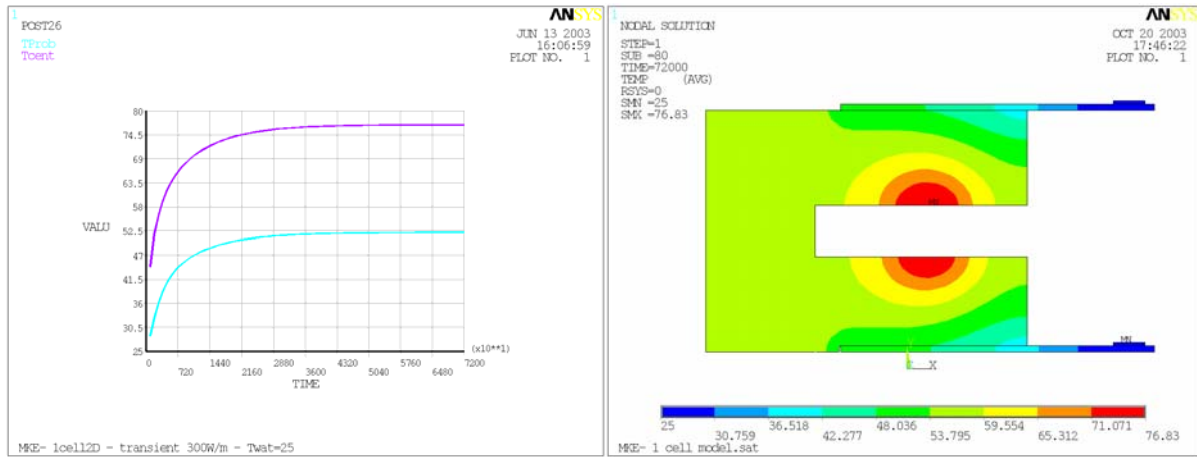


Figure 15 Ansys® results

4.5.3 Time constants

With Ansys® several simulations have been made of the temperature as a function of time, similar as the one shown in figure 15. Time constants have been calculated for different conditions and for different probe positions. The resulting time constants are presented in Appendix B. For the calculation of the time constants, the temperatures are fitted to an exponential, over a period of 14 hours. As shown in the appendix, the calculations are done for different heating powers, warm-up and cool-down, and for different positions on the ferrite. For the nominal ferrite density of 5 kg/dm^3 all time constants are between 3.4 hours and 4.2 hours. For the smaller (non realistic) ferrite density of 3.5 kg/dm^3 the time constants are in general almost one hour smaller.

This can be compared with the time constants measured on the cooling test bench, as described in chapter 4. The measured time constants for the test bench, also exponentially fitted over 14 hours, vary between 5.1 hours and 5.4 hours for the heating, depending on the temperature probe. For the cool down the time constant is about 7 hours.

For the complete magnet installed in the SPS the cool-down time constants have been measured, after been heated by the beam. These values, also calculated over 14 hours, vary between 12 hours and 14 hours. With the water-cooling switched off, the cool-down time constant increases to about 26 hours. At the moment it is unclear why the time constant of a complete magnet in the machine is that much larger than the time constant of the laboratory test bench and its simulation.

5. MACHINE MEASUREMENTS

The validity of the models presented in the previous chapters can best be judged by measurements of the kicker field strength performed in the SPS.

In order to verify the calculated values, the kick strength of a MKE magnet has been evaluated by analysing the kicker induced beam with the SPS “1000 turn” measurement system. The results are shown in figure 16. It can be observed that the kick strength starts diminishing from 80 °C (measured with the temperature sensors) onwards. According to the simulations with Design Space[®], (see figure 10), this corresponds to a ferrite temperature of 125 °C i.e. to the Curie temperature of the ferrite and confirms the correctness of the model.

Similar measurements have been performed on the MKQH magnet, which has a similar design but has neither been equipped with water-cooling nor temperature sensors. The corresponding temperatures have been measured on the MKE magnet. The decline of the kick strength starts from about 50°C degrees onwards. Assuming a linear relation between heating power of the beam and temperature rise in the ferrite, it can be concluded that the cooling system allows the magnet to be operational with approximately double the beam deposited heating power.

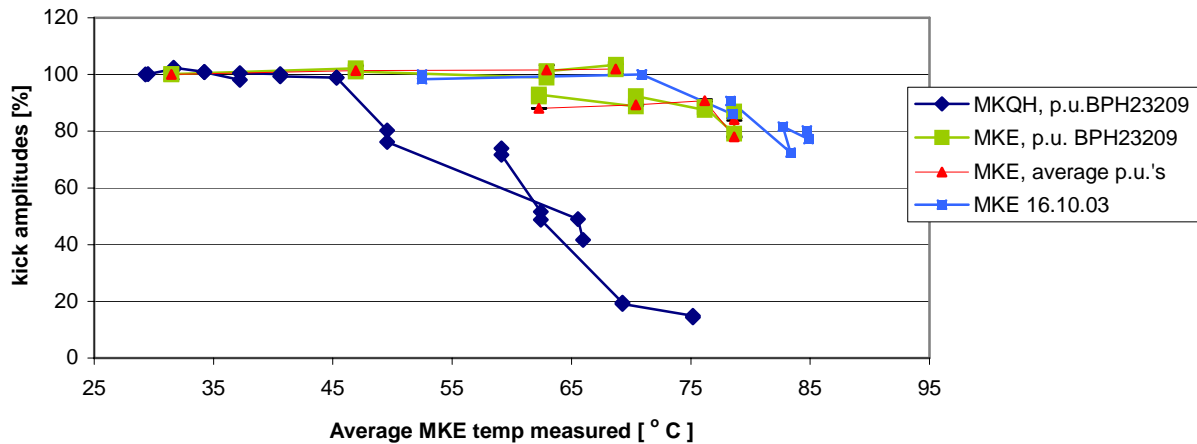


Figure 16 Measured kicker field strength for the MKE kicker magnet and the MKQH kicker magnet as a function of the measured MKE temperature.

6. CONCLUSIONS AND DISCUSSION

The modified MKE kicker magnets have been equipped with a water cooling system in order to limit the temperature rise due to beam induced heating. The aim is to keep the ferrite temperatures below the Curie temperature. Finite element simulations with Design Space[®] predict temperatures of the ferrites, close to the circulating beam, which agree within 5 % with the measurements performed at the test bench. These results are also confirmed by measured temperatures and kick strengths on the operational modules in the SPS. However, significant temperature differences have been found between the calculated and the measured temperatures in other position of the ferrite cross-section. This is most likely due to certain assumptions in the calculations concerning the material properties, the values of heat transfer and thermal contact of the temperature probes. Further investigations with more refined models and more precise values for the material properties could improve these simulations significantly.

Additionally, heating and cool-down of the system were calculated with Ansys[®]. The calculated value for the heating time corresponds well with the test-bench measurements. However, significant differences were found in the values for the cool-down constants. Although the calculations showed 4 hours for a given temperature drop, the measurements in the lab required 7 hours and 13 hours were required in the SPS machine. At the moment this difference is not understood.

Although the modelling of the MKE cooling system leaves some questions open, the most important parameter, the highest temperature in the ferrite and its relation to the probe temperature for the machine model, seems to be accurate. The conceptual design of the cooling system was approved and the series production was launched. The magnets were installed and perform according to the specifications of the cooling system.

7. ACKNOWLEDGEMENT

The author would like to thank J.Uythoven, T. Kurtyka, M. Mayer, L. Ducimetière G. Arduini for their help and fruitful discussions.

APPENDIX A: ALUMINIUM NITRIDE CHARACTERISTICS

Aluminium Nitride			AlN 180
ρ_{th}	Density (theoretical)	(g/cm ³)	3.32
ρ_m	Density (as measured)	(g/cm ³)	3.31
σ_B	Flexural strength	(MPa)	> 300
σ_D	Compressive strength	(GPa)	> 2.0
K_{IC}	Fracture toughness	(MPa m ^{1/2})	3.35 ± 0.2
E	Young's modulus	(GPa)	310
λ	Thermal conductivity	(W/mK)	180 ± 10
α	Coeff. of thermal expansion	(10 ⁻⁶ K ⁻¹)	
	RT - 100 °C		3.6
	RT - 1000 °C		5.6
c_p	Specific heat	(J/kgK)	738 ± 20
	Volume resistivity	(Ω cm)	> 5 x 10 ¹²
	Dielectric strength	(kV/mm)	> 20
ϵ_r	Dielectric constant	(at 1 MHz)	8.6
	Resistance to thermal shock		excellent

APPENDIX B: HEATING TIME CONSTANTS

Different time constants calculated from Ansys® calculations. The different ferrite densities used only result in a different time constant but not in different equilibrium temperatures.

<i>Temperature location</i>	<i>Ferrite density [kg/dm³]</i>	<i>Exponential time constant τ [hours]</i>	<i>Condition</i>
Core position	5	4.1	Increase power from 0 W/m to 200 W/m
	3.5	3.5	Idem
Probe position	5	3.8	Idem
	3.5	3.1	Idem
Top ferrite	5.0	3.9	Idem
	3.5	3.0	Idem
Core position	5	4.0	Increase power from 200 W/m to 412 W/m
	3.5	3.4	Idem
Probe position	5	3.8	Idem
	3.5	3.1	Idem
Top ferrite	5.0	4.0	Idem
	3.5	3.1	Idem
Core position	5	4.2	Increase power from 412 W/m to 846 W/m
	3.5	3.7	Idem
Probe position	5	3.8	Idem
	3.5	3.2	Idem
Top ferrite	5.0	4.2	Idem
	3.5	3.4	Idem
Core position	5.0	3.5	Cool-down form 846 W/m to zero heating
	3..5	2.5	
Probe position	5.0	3.4	
	3..5	2.5	
Top ferrite position	5.0	3.8	
	3..5	2.7	

Distribution list

Laurent Ducimetière, Volker Mertens, Enrique Gaxiola, Cristoforo Benvenuti, Tadeusz Kurtyka, Manfred Mayer, Karel Cornelis, Paul Collier, Konrad Elsener, Brennan Goddard, Gianluigi Arduini, Jörg Wenninger.